Mesoscopic Kondo effects in nanoscale systems

Mahn-Soo Choi

Department of Physics,
Korea University, Seoul 136-701, Korea
E-mail: choims@korea.ac.kr

Abstract: A few selected topics on the Kondo effects in mesoscopic systems have been reviewed. Included are the effects of the competition of the spin polarisation and the superconductivity with the Kondo correlation in quantum dots coupled to ferromagnetic and superconducting leads, respectively, and the SU(4) Kondo effects due to the orbital degeneracy in vertical quantum dots, carbon nanotube quantum dots, and lateral double quantum dots.

Keywords: Kondo effect; quantum dot; nanostructure; magnetic impurity; numerical renormalisation group; scaling theory.

Reference to this paper should be made as follows: Choi, M-S. (2006) 'Mesoscopic Kondo effects in nanoscale systems', *Int. J. Nanotechnology*, Vol. 3, Nos. 2/3, pp.216–235.

Biographical notes: Mahn-Soo Choi received a BSc in Physics in 1993, a Master Degree in Physics on vortex excitations in low dimensional phase transitions in 1995, and a PhD in Physics on quantum phase transitions and dynamical properties of Josephson-junction arrays from the Pohang University of Science and Technology in Korea in 1998. Thereafter, he joined the University of Basel in Switzerland as a Postdoctoral Researcher, where extended his research interest to the quantum transport in mesoscopic systems and the physical implementation of quantum information processing with solid-state systems. In 2000, he moved back to Seoul to work as a Research Fellow at Korea Institute for Advanced Study (KIAS). Since 2002, he is a Faculty Member of the Department of Physics at Korea University in Seoul, Korea. He is also an Associate Member of KIAS.

1 Introduction

Magnetic impurities embedded in metallic hosts cause anomalous resonant scattering of conduction electrons. Further, the localised magnetic moments of the impurities are screened at low temperatures by the itinerant electron spins. Such an effect is called the Kondo effect, one of the most extensively studied subjects in condensed-matter physics [1,2].

Ever since the theoretical predictions [3,4] and the experimental demonstrations [5–9], the Kondo effect has been revived recently in phase-coherent mesoscopic systems and has stimulated great-renewed interest in this field [10]. The main support of this remarkable success is the tunability in the mesoscopic systems. The fine tunability enables to test various aspects of the Kondo effect that cannot be directly investigated in bulk solids. For example, a scattering phase shift at the Kondo resonance in a quantum dot has been measured using a two-path interferometer [8].

The controlled manipulation in mesoscopic systems has also posed further exciting issues. Among many other examples are the competitions of the spin-dependent transport (Section 2) and the superconducting correlation (Section 3) with the Kondo correlation and the interplay of the orbital and the spin Kondo effects (Section 4), whose recent experimental and theoretical developments will be reviewed in subsequent sections. This review should not be regarded in any respect as a complete review of the mesoscopic Kondo effects. Rather we will focus on a few special topics. Some important examples of issues that are left for a more complete review include the anomalous transmission phase shift through the quantum dot in the Kondo regime [8,11,12], the singlet-triplet Kondo effects in quantum dots with even number of electrons [13–21], and the Kondo screening cloud [22,23].

The paper is organised as following: In Section 2, the Kondo effects in the quantum dot coupled to ferromagnetic leads will be reviewed, focusing on the theoretical debates and recent experiments. Section 3 is devoted to discuss the Josephson current through a quantum dot in the Kondo regime and the $0 - \pi$ transition as a function of the ratio of the superconducting gap and the Kondo temperature. In Section 4, we will review the orbital Kondo effects on vertical quantum dots, carbon nanotube quantum dots, and parallel double dots, where one tune the crossover between the SU(2) and SU(4) Kondo effects.

2 Quantum dots coupled to ferromagnetic leads

A flood of very recent works [24–36] has addressed an interesting issue, namely, how the Kondo physics is affected when the continuum electrons themselves are allowed to form *spin-dependent* bands. The motivation for this research stems from the successful field of spintronics [37]. In particular, a change has been detected in the resistivity of a Kondo alloy due to spin-polarised currents [38]. Furthermore, it is already possible to attach ferromagnetic leads to a carbon nanotube [39], and a carbon-nanotube QD has been shown to display Kondo physics below an unusually high temperature [40]. In addition, a QD coupled to ferromagnetic electrodes has been proposed as a promising candidate for spin injection devices, but until very recently, analysed only in the Coulomb blockade regime [41].

Recent studies of QDs coupled to ferromagnetic leads in the strong coupling regime (Kondo regime) raised a controversy in the literature with regard to whether a spin-dependent renormalisation of the impurity level induced by the spin-polarised leads will split the Kondo peak when the magnetic moments of both leads are aligned. In Sergueev et al. [35], an equation-of-motion (EOM) method plus an ansatz for the interacting self-energy [42] were employed and it was suggested that the splitting, Δ_K, is absent. In a later work [32], the scaling arguments (together with the EOM method) were used to find that Δ_K is nonzero. In Zhang et al. [36], using a similar approach, a splitting was predicted only in the mean-field peaks. In a more recent work [26], they made use of a noncrossing approximation (NCA) and obtained $\Delta_K \neq 0$. In Bułka and Lipiński [24] and López and Sánchez [27], on the other hand, the slave-boson mean-field theory (SBMFT) was utilised to study the zero-temperature properties and no splitting was observed. The answer to the controversy is, thus, elusive because each approximation method mentioned above has certain drawbacks of its own.

The controversy was resolved in Choi et al. [25] and Sánchez et al. [34] using the numerical renormalisation group (NRG) method [43–49]. They (and independently the authors in Martinek et al. [31]) also investigated the influence of ferromagnetic electrodes and the relative orientations of their magnetisations on the equilibrium properties of a QD with and without intrinsic spin flip processes, across the different parameter regimes (i.e., Kondo, mixed-valence, and empty-orbital), thoroughly analysed with the assessment of local DOS, linear conductance, and tunnelling magneto resistance (TMR). The theoretical results have been confirmed in a recent experiment [33] on C_{60} molecules coupled to ferromagnetic nickel electrodes. The effect of the detailed band structure on the splitting of the Kondo peak in the presence of the ferromagnetism was further investigated in Martinek et al. [30].

The system consists of ultra small tunnel junctions between a QD and two ferromagnetic leads. It is assumed that the QD has a localised energy level with an unpaired spin-1/2 electron and a charging energy U. This way, the QD is equivalent to an Anderson-type impurity with single-particle energy $\varepsilon_{d,\sigma}$ for spin $\sigma = \{\uparrow, \downarrow\}$ [3,4]. Notice that $\varepsilon_{d,\sigma}$ includes the Zeeman energy $\Delta_Z \equiv \varepsilon_{d,\uparrow} - \varepsilon_{d,\downarrow}$ due to the magnetic field from an external magnet and possibly from the ferromagnetic leads. In what follows, we set $\Delta_Z = 0$ in order to unmask the spin-dependent normalisations of the bare energy level purely due to coupling with the leads [50]. Tunnelling of electrons from the QD to the leads (reservoirs) $\alpha = \{L, R\}$ is described by the hopping integral $V_{\alpha k\sigma}$. The resulting Hamiltonian is given by:

$$H = \sum_{\sigma} \varepsilon_{d,\sigma} \hat{n}_{\sigma} + U \hat{n}_{\uparrow} \hat{n}_{\downarrow} + R\left(d_{\uparrow}^{\dagger} d_{\downarrow} + \text{H.c.}\right) + \sum_{\alpha k \sigma} \left[\varepsilon_{\alpha k\sigma} c_{\alpha k\sigma}^{\dagger} c_{\alpha k\sigma} + (V_{\alpha k\sigma} c_{\alpha k\sigma}^{\dagger} d_{\sigma} + \text{H.c.}) \right], \quad (1)$$

where $c_{\alpha k\sigma}^{\dagger}(c_{\alpha k\sigma})$ is the creation (annihilation) operator for an electron with wave vector k and spin in the electrode α. The QD occupation number is $\hat{n}_{\sigma} = d_{\sigma}^{\dagger} d_{\sigma}$ [$d_{\sigma}^{\dagger}$ (d_{σ}) creates (annihilates) an electron in the dot].

For definiteness, leads are assumed to be identical, with chemical potentials $\mu_L = \mu_R = E_F$ and symmetric couplings. Ferromagnetism on the leads may be represented either by a spin-dependent DOS $\rho_{\alpha\sigma}(\omega)$ or by spin-dependent tunnelling amplitudes $V_{\alpha k\sigma}$. Both pictures are formally equivalent as far as the transport properties are concerned. In any case, the overall effect results in a spin-dependent hybridisation parameter $\Gamma_{\alpha\sigma}(\omega) \equiv \pi \sum_k |V_{\alpha k\sigma}|^2 \, \delta(\omega - \varepsilon_{\alpha k})$. As usual, proximity effects such as stray fields induced in the QD and the energy dependence of $\Gamma_{\alpha\sigma}(\omega)$ are neglected. In the following, we choose $E_F = 0$ as the origin of energies. One can define the spin polarisation (close to the Fermi energy) at each lead as $p_{\alpha} = (\Gamma_{\alpha\uparrow} - \Gamma_{\alpha\downarrow})/(\Gamma_{\alpha\uparrow} + \Gamma_{\alpha\downarrow})$ with $-1 \le p_{\alpha} \le 1$. We consider parallel (P) and antiparallel (AP) magnetisations of the two leads. In the P case ($p_L = p_R \equiv p$), we have $\Gamma_{L\uparrow} = \Gamma_{R\uparrow} = (1 + p)\Gamma_0/2$ and $\Gamma_{L\downarrow} = \Gamma_{R\downarrow} = (1 - p)\Gamma_0/2$, where $\Gamma_0 \equiv \Gamma_{\alpha\uparrow} + \Gamma_{\alpha\downarrow}$, whereas the AP case ($p_L = -p_R \equiv p$) yields $\Gamma_{L\uparrow} = \Gamma_{R\downarrow} = (1 + p)\Gamma_0/2$ and $\Gamma_{L\downarrow} = \Gamma_{R\uparrow} = (1 - p)\Gamma_0/2$.

Various methods [24–36] have been used to obtain the local spectral density of single-particle excitations (or, simply DOS, density of states) $A_{\sigma}(\omega)$ with spin σ. Notice that all the physics (correlations, dependence on the gate voltage, etc.) is contained in $A_{\sigma}(\omega)$. The linear conductance (normalised to e^2/h) of the junction at zero temperature is

obtained from the impurity spectral density function at the Fermi level [51], $g = \sum_\sigma 2\Gamma_{L\sigma}\Gamma_{R\sigma}A_\sigma(0)/(\Gamma_{L\sigma}+\Gamma_{R\sigma})$.

Figure 1 shows $A_\uparrow(\omega)$, $A_\downarrow(\omega)$, and $A(\omega) = A_\uparrow(\omega) + A_\downarrow(\omega)$ for different values of the lead polarisation p in the P configuration (the AP case is less interesting as both spin orientations are equally coupled). Left panels correspond to the symmetric Anderson model (i.e., $\varepsilon_d = -U/2$). For $p = 0$, in addition to two (symmetric) mean-field peaks at $\omega = \varepsilon_d$ and $\omega = \varepsilon_d + U$, $A(\omega)$ shows a peak at $\omega = 0$ [see Figure 1(a)], which is responsible for the observed zero-bias anomaly. As p increases, the spectral peak of $A_\uparrow(\omega)$ [$A_\downarrow(\omega)$], at the Fermi energy increases (decreases). Remarkably, however, the central peaks of both $A_\uparrow(\omega)$, and $A_\downarrow(\omega)$, are pinned at the Fermi level; in particular, the Kondo peak in $A(\omega)$, does *not* split. Experimentally, one would see a perfect transparency of the junction (see below). Right panels of Figure 1 show the same functions for the asymmetric case ($\varepsilon_d \neq -U/2$), where charge fluctuations are allowed to certain extent. As p increases, $A_\uparrow$ and $A_\downarrow$ shift in opposite directions [see Figure 1(b)] and the Kondo peak in $A(\omega)$ splits into two. As a result, the Kondo effect is suppressed. One can checked as well that both mean-field peaks are shifted in opposite directions.

Figure 1 Local DOS of the QD for (a) the symmetric Anderson model and (b) the asymmetric Anderson model. Plotted are $A_\uparrow(\omega)$ (top), $A_\downarrow(\omega)$ (middle), and $A(\omega)$ (bottom) for $\varepsilon_d = -U/2 = -0.1D$ and $\Gamma_0 = 0.02D$, where D is the bandwidth)

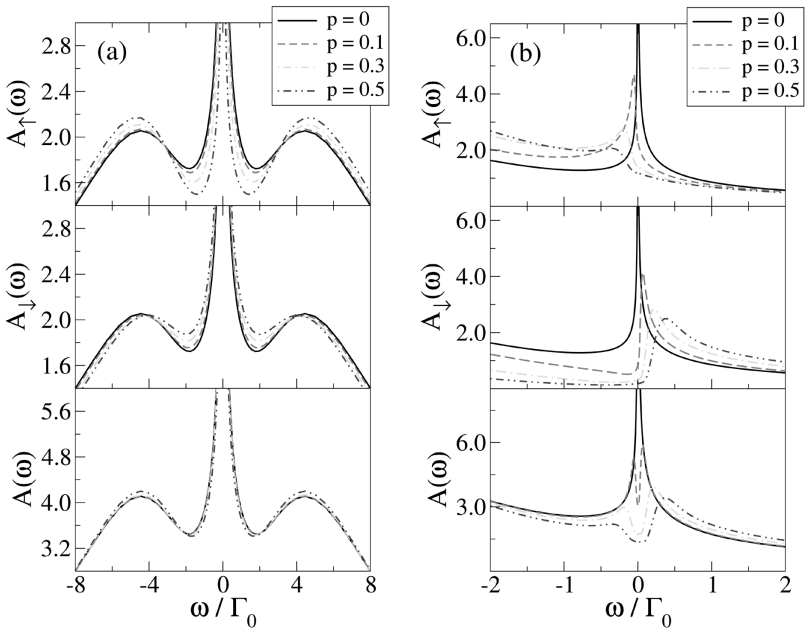

The finite splitting for the asymmetric Anderson model may be understood in terms of simple scaling arguments [32]: Because the hybridisation for up spins is larger than for down spins ($\Gamma_{\alpha\uparrow} > \Gamma_{\alpha\downarrow}$), the renormalisation of the bare level ε_d is spin-dependent; the $\uparrow(\downarrow)$-electron lowers (raises) its energy. Then, the coupling acts as an effective magnetic field, leading to a finite Δ_K [52]. Yet, the perturbative nature of a poor man's scaling cannot describe the fixed point in the strong coupling regime. In particular, such simple

scaling arguments cannot account properly for the particle-hole symmetry in the symmetric Anderson model and always predict $\Delta_K \neq 0$. For the symmetric Anderson model, it is important to notice that the particle-hole symmetry quenches charge fluctuations completely for both spins ($\langle n\uparrow \rangle = \langle n\downarrow \rangle = 1/2$) at *any* $|p| < 1$, and the real part of the self-energy (at E_F) is zero. This means that although the binding energy of the singlet state (the Kondo temperature T_K) diminishes with p, the quasiparticle lifetime is still infinite and the Fermi liquid picture is valid. Therefore, the results in Figure 1(a) are consistent with SBMFT, which describes the Kondo peak when spin fluctuations prevail. Likewise, the results in Figure 1(b) are in agreement with EOM and NCA models, which support charge fluctuations to some degree. Of course, the NRG method can encompass the whole parameter range.

To illustrate the conclusions above, Choi et al. [25] measured the splitting Δ_K of the Kondo peak as a function of ε_d (experimentally this is controlled by a gate voltage) with U fixed [see Figure 2(a)]. The splitting Δ_K increases roughly linearly from zero as moving away from the symmetric point $\varepsilon_d = -U/2$. Notice also that well away from $\varepsilon_d = -U/2$, Δ_K is linear in the lead polarisation [see Figure 2(b)], confirming the prediction relying upon scaling arguments.

Figure 2 The splitting Δ_K of the Kondo peak in the local spectral density $A(\omega)$ as a function of (a) the impurity level position ε_d and (b) the polarisation P

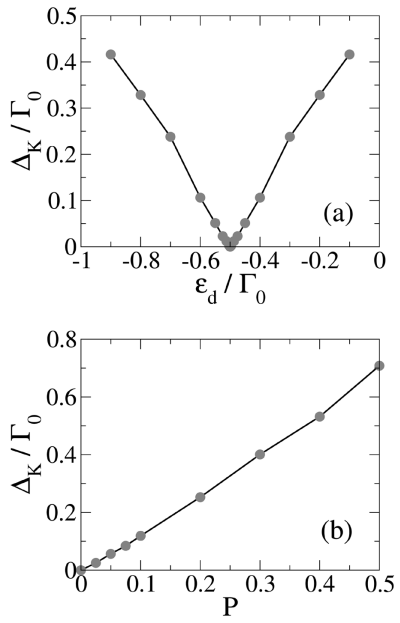

We now turn to the tunnelling magnetoresistance, TMR = $(g^{\mathrm{P}} - g^{\mathrm{AP}})/g^{\mathrm{AP}}$ as reported in Choi et al. [25]. Here $g^{\mathrm{P}} = \pi\Gamma_0[(1+p)\,A\uparrow(0) + (1-p)\,A\downarrow(0)]$ and $g^{\mathrm{AP}} = (1-p^2)\,\pi\Gamma_0\,A(0)$ are the dimensionless linear conductance for the P and AP configurations, respectively. For the symmetric Anderson model, the Kondo effect survives even for a finite value of polarisation $p\,(|p| < 1)$, and g^{P} preserves the unitary limit. As a result, the TMR is given by TMR = $p^2/(1-p^2)$. For the asymmetric Anderson model, on the contrary, g^{P} gets

strongly suppressed as p increases and the system exhibits a strong negative TMR [53]; see Figure 3(b). Figure 3(a) shows TMR as a function of ε_d, which shows a sharp peak around the symmetry point ($\varepsilon_d \simeq -U/2$). The width of the peak is determined by how fast the Kondo effect is suppressed as $\left|\varepsilon_d - U/2\right|$ increases from zero, and hence depends strongly on the polarisation p and the hybridisation Γ_0; see Figure 2(a) and 2(b). Experimentally, finite temperatures would smoothen this peak.

Figure 3 TMR as a function of (a) the impurity level position ε_d for P = 0.5 and (b) the polarisation P

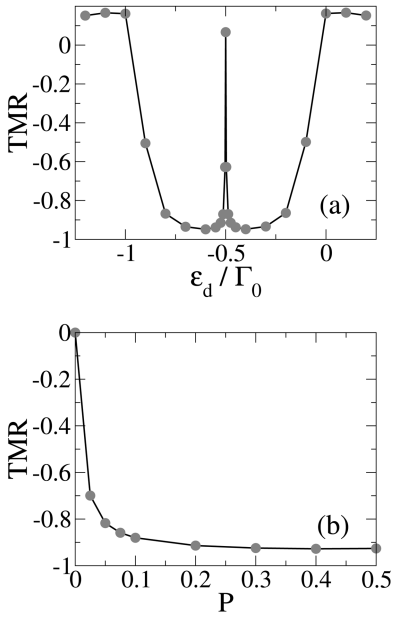

3 Kondo enhanced Josephson current

The Kondo effect and superconductivity are two of the most extensively studied phenomena in condensed matter physics ever since the pioneering works by Kondo [2] and by Bardeen et al. [54], respectively. When a localised spin is coupled to superconducting electrons, the two effects are intermingled and even richer physics emerge. Physically interesting questions are: Would the Kondo effect survive, overcoming the spin-singlet pairing of electrons in superconductors (SCs) and the superconducting gap at the Fermi level? If it does, how would such a strongly correlated state affect the transport, especially the Josephson current, between two superconductors?

The Josephson effect through a strongly interacting region with a localised spin was discussed long before by Shiba and Soda [55] and Glazman and Matveev [56] and further elucidated by Spivak and Kivelson [57]. The large on-site interaction only allows the electrons in a Cooper pair to tunnel one by one via virtual processes in which the spin ordering of the Cooper pair is reversed, leading to a negative Josephson coupling (i.e., a π-junction). This argument, however, is based on a perturbative idea and holds true only for sufficiently weak tunnelling. It was suggested [56] that as the tunnelling increases, the

Kondo effect produces a collective resonance at the Fermi level. As a result, the Josephson current is enhanced by the Coulomb repulsion. Moreover, the Josephson coupling is expected to be positive (i.e., a 0-junction) since the localised spin is screened due to the Kondo effect. Based on this, Glazman and Matveev [56] assumed a strong coupling fixed point and derived the Josephson current as a function of phase difference. Recently, several approximation methods have been used to investigate the transition from the 0- to π-junction as a function of the tunnelling strength [58–61]: A modified Hartree-Fock approximation [59], a non-crossing approximation (NCA) [58], and a variational method [60] predict a 0–π transition, whereas the slave-boson mean-field theory [60] always favours the Kondo effect.

More thorough and accurate studies of the 0–π transition and associated Josephson current have been reported very recently based on a NRG method [62–64] (see Yoshioka and Ohashi [65] for an extension of the NRG method to the case of superconducting leads) and Quantum Monte Carlo simulation [66] (see also Choi et al. [63], Siano and Egger [67] for refinement of the interpretations of the results in Siano and Egger [66]). Buitelaar et al. [68] measured experimentally the linear and non-linear conductance in SC-carbon nanotube-SC junctions in the Kondo regime.

The system in question consists of a QD with an odd number of electrons coupled to two superconducting leads (L and R). The two leads are regarded to be standard s-wave superconductors (SCs) and described by the BCS Hamiltonian

$$H_{\mathrm{BCS}} = \sum_{\ell=L,R} \sum_{\mathbf{k},\sigma} \varepsilon_{\ell,\mathbf{k}} c^{\dagger}_{\ell,\mathbf{k},\sigma} c_{\ell,\mathbf{k}\sigma} - \sum_{\ell} \sum_{\mathbf{k}} \left(\Delta_{\ell} e^{+i\phi_{\ell}} c^{\dagger}_{\ell,\mathbf{k},\uparrow} c^{\dagger}_{\ell,-\mathbf{k},\downarrow} + h.c. \right), \tag{2}$$

where $c^{\dagger}_{\ell,\mathbf{k},\sigma}(c_{\ell,\mathbf{k},\sigma})$ creates (destroys) an electron with energy $\varepsilon_{\ell,\mathbf{k}}$, momentum $\hbar\mathbf{k}$, and spin σ on the lead ℓ. Δ_{ℓ} is the superconducting gap and ϕ_{ℓ} is the phase of the superconducting order parameter. The QD is described by an Anderson-type impurity model

$$H_{\mathrm{QD}} = \sum_{\sigma} \varepsilon_d d^{\dagger}_{\sigma} d_{\sigma} + U d^{\dagger}_{\uparrow} d_{\uparrow} d^{\dagger}_{\downarrow} d_{\downarrow}, \tag{3}$$

which is widely adopted for sufficiently small quantum dots. In equation (3) $d^{\dagger}_{\sigma}$ and d_{σ} are electron creation and annihilation operators on the QD. The level position ε_d, measured from the Fermi energy E_F of the two leads (throughout the paper every energy is measured from E_F), can be tuned by an external gate voltage. The interaction U is order of charging energy $e^2/2C$ (C is the capacitance of the QD). The coupling between the QD and the SCs is described by the tunnelling Hamiltonian

$$H_V = \sum_{\ell} \sum_{\mathbf{k},\sigma} V_{\ell} \left(d^{\dagger}_{\sigma} c_{\ell,\mathbf{k},\sigma} + h.c. \right). \tag{4}$$

Putting all together the Hamiltonian for the whole system is given by $H = H_{QD} + H_{\mathrm{BCS}} + H_V$.

For simplicity, the two SCs are assumed to be identical ($\varepsilon_{L,\mathbf{k}} = \varepsilon_{R,\mathbf{k}} = \varepsilon_{\mathbf{k}}$ and $\Delta_L = \Delta_R = \Delta$, see Oguri et al. [64] for a discussion in the asymmetric case) except for a finite phase difference $\phi = \phi_L - \phi_R$; without loss of generality we put $\phi_L = -\phi_R = \phi/2$. In the normal state, the conduction bands on the leads are symmetric with a flat density of states N_0 and the width D above and below the Fermi energy. We also put $\varepsilon_d = -\mathrm{U}/2$ in

H_{QD}, equation (3); one can check that an asymmetric model ($\varepsilon_d \neq -U/2$) gives the qualitatively same results. Only symmetric junctions are considered, $V_L = V_R = V$. The coupling to the leads is well characterised by the single parameter $\Gamma = 2\pi N_0 V^2$. The strong ($T_K \gg \Delta$) and the weak ($T_K \ll \Delta$) coupling limits is characterised by the ratio of the superconducting gap Δ to the *normal-state* Kondo temperature $T_K(k_B = 1)$ given by [69]

$$T_K = \Gamma\sqrt{\frac{U}{2\Gamma}}\exp\left[\pi\frac{\varepsilon_d}{2\Gamma}\left(1+\frac{\varepsilon_d}{U}\right)\right]. \tag{5}$$

How superconductivity on the leads affects the interacting QD in the strong and weak coupling limits is already reflected in the local properties on the QD with zero phase difference ($\phi = 0$). Figure 4 shows the local pair correlation $\Delta_d \equiv \left\langle d_\uparrow^\dagger d_\downarrow^\dagger \right\rangle$ as a function of Δ/T_K. As expected, the local pair correlation Δ_d vanishes with Δ, and gets smaller (even vanishes when $U \to \infty$) as $\Delta \to \infty$; see Figure 4 (inset). An interesting aspect of Δ_d is the sign change at $\Delta = \Delta_c \simeq 2.4T_K$, which suggests that the physical properties are different in the strong ($T_K \gg \Delta$) and the weak ($T_K \ll \Delta$) coupling limits. Indeed one can be convinced (from the NRG calculation [62] or the variational studies [60]) that the ground-state wave function of the whole system is of spin singlet (the localised spin is screened out) for $\Delta < \Delta_c$ and of spin doublet (the SCs form Cooper pairs separately and the localised spin is left unscreened) for $\Delta < \Delta_c$. The negative sign in Δ_d in the weak coupling limit can be explained by a simple second-order perturbation theory, while the positive on in the strong-coupling limit is expected when there is a resonance channel for Cooper-pair tunnelling [70]. This feature can also be interpreted by means of the Andreev bound states crossing the Fermi level with the increasing Δ/T_K; see Clerk et al. [71], Clerk and Ambegaokar [58].

Figure 4 Gap of the local quasiparticle excitations

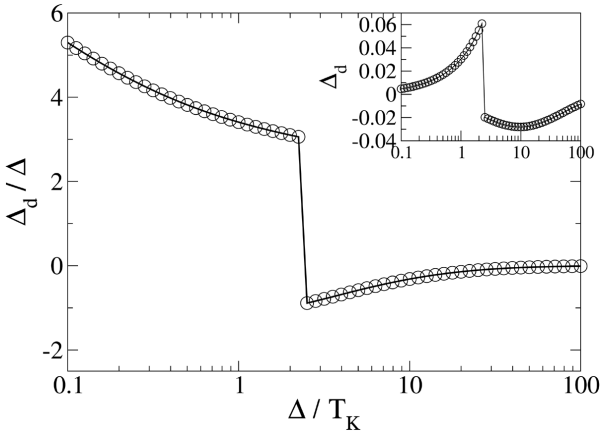

We now turn to the Josephson current through the QD in the presence of a finite phase difference ϕ. Figure 5 shows the Josephson current as a function of phase difference ϕ between the two superconducting leads for different values of ratio Δ/T_K. In the weak coupling limit ($T_K \ll \Delta$), it is clearly seen from Figure 5(a) that the effective Josephson

coupling is negative (i.e., a π-junction) [55–58,72]. In addition, the supercurrent-phase relation is very close to a sinusoidal function, like typical 'tunnelling junctions' [70]. It was also noticed that the ground state is a doublet for any phase difference ϕ.

Figure 5 Josephson current $I_S(\phi)$ (in units of $I_c^{short} \equiv e\Delta/\hbar$) as a function of phase different ϕ (a) for $\Delta/T_K = 10$ and (b) for $\Delta/T_K = 0.1$. (c) Same curves for $\Delta/T_K = 1.6$, 1.8, 2.0, and 2.2 (near the $0 - \pi$ junction transition point)

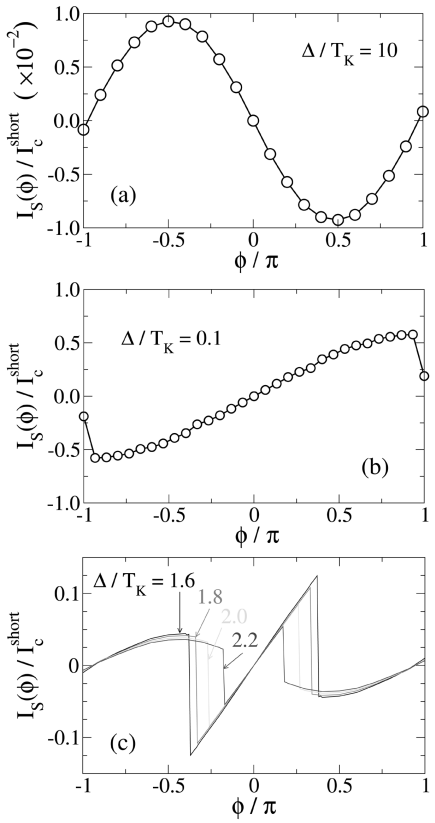

In the strong coupling limit ($T_K \gg \Delta$), on the other hand, the Josephson coupling is positive [58–60]; see Figure 5(b). Another remarkable thing is that the current-phase relation is highly non-sinusoidal and reminiscent of the current-phase relation in the short junction limit [70]. Furthermore, the critical current approaches the unitary limit I_c^{short} of 'short junctions' [70] as the coupling grows stronger ($\Delta/T_K \to 0$), as shown in Figure 6. These results suggest again that in the strong coupling limit the Kondo resonance develops at the Fermi level and Cooper pairs tunnel resonantly through it. Naturally, the ground state turns out to be a spin singlet for any ϕ.

Another interesting regime is the intermediate one ($\Delta \sim T_K$). As demonstrated in Figure 5(c), for $\Delta \sim T_K$ the curve of $I_S(\phi)$ breaks into three distinct segments. The central segment resembles that of a ballistic short junction [70], while the two surrounding segments are parts of a π-junction curve [59]. Namely, the critical value $\Delta_c(\phi)$ depends on

ϕ with $\Delta_c(\phi) > \Delta_c(\phi')$ for $|\phi| < |\phi'|$ [73,74]; for example, $\Delta_c(0.3\pi) \approx 1.6$ and $\Delta_c(0) \approx 2.4$. Evidently, the NRG results show that the ground state is a spin singlet in the central segments ($\Delta < \Delta_c(\phi)$) and a doublet in the other ($\Delta > \Delta_c$).

Figure 6 Critical current in the Kondo regime. We put $\varepsilon_d = -U/2 = -0.1D$ and $\Gamma = 0.04D$. Inset: conductance resulting from the RSJ-model (see text)

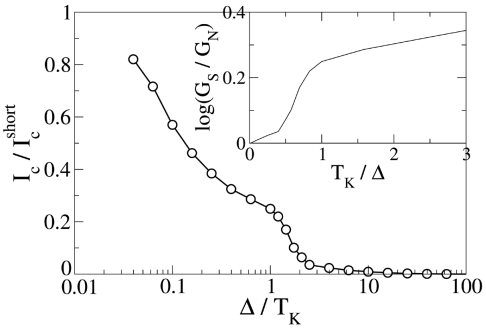

In the experiments of Buitelaar et al. [68] the interplay between superconductivity and Kondo physics was observed in non-equilibrium transport (multiple Andreev reflections) [75,76], but no supercurrent was measured. The absence of dissipation less branch in the IV is not surprising in such (intrinsically) small junctions. Indeed thermal or quantum fluctuations in connection with a resistive environment can lead to a finite resistance [77]. The numerical results in Choi et al. [62] are in qualitative agreement with the crossover of the conductance in the experiment [see Figure 6 (inset)], and further analysis is required [78].

So far, there is no experiment where the Josephson current in the Kondo regime is directly measured. A possible experimental setup for direct measurement of the Josephson current in the Kondo regime is a superconducting loop interrupted with the quantum dot (see Figure 7), which was successfully used to measure the spontaneous supercurrent through the superconductor-ferromagnet-superconductor junctions in the Kondo regime [79].

Figure 7 The superconducting loop interrupted with the quantum dot as a possible experimental setup to measure directly the Josephson current in the Kondo regime; see Bauer et al. [79]. Here the carbon nanotube serves as a quantum dot. Measurement of the flux induced in the loop gives the Josephson current through the quantum dot

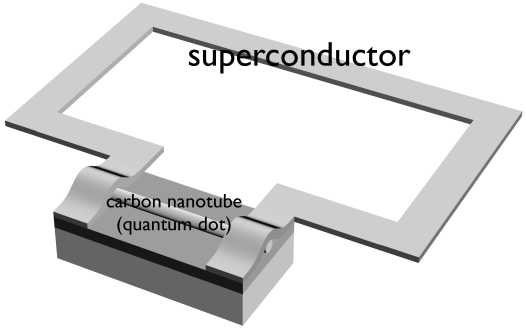

4 SU(4)-symmetric orbital and spin Kondo effects

In the previous sections, we have discussed Kondo effects through single localised levels in artificial Kondo impurities, focusing on the roles of unusual electrodes. A natural step forward is the understanding of the interaction between the two or more localised orbital levels in the Kondo regime, which is the subject of the present section. The relevant orbital states may be either in the same Kondo impurity [80–83] or separately in respective Kondo impurities [84–86]. In this case, the orbital degrees of freedom also come into play as a pseudo-spin, giving rise to exotic physical scenarios [87–90]. In particular, when the interdot Coulomb interaction is large, the Kondo correlated state possesses a SU(4) symmetry involving both the (real-)spin and pseudo-spin [91,92], and the Kondo effect is enhanced. Similar physics emerges on other QD-related structures as well [93].

Natural prototype models for studying the interplay between the orbital pseudospin and real spin degrees of freedom are provided by the vertical quantum dot [see Figure 8(a)], the carbon nanotube quantum dot [Figure 8(b)], and the double quantum dot [Figure 8(c)] on the two-dimensional electron systems. The vertical quantum dot systems have been studied extensively as a tunable single-electron devices [9,20,82,83,94] as the electronic states, in particular, the orbital degeneracy between them can be easily tuned via external gate voltage. Carbon nanotubes (NTs) also exhibit a good deal of remarkable transport phenomena including quantum interference [95], Luttinger liquid features [96] or spin polarised transport [39]. Finite-length NTs behave like quantum dots (QDs) and thus show Coulomb blockade and Kondo physics [40,97,98]. The electronic states of a NT form one-dimensional electron and hole sub-bands. They originate from the quantisation of the electron wavenumber perpendicular to the nanotube axis, $k_\perp$, which arises when graphene is wrapped into a cylinder to create a NT. By symmetry, for a given sub-band at $k_\perp = k_0$ there is a second degenerate sub-band at $k_\perp = -k_0$. Semiclassically, this orbital degeneracy corresponds to the clockwise (↻) or counterclockwise (↺) symmetry of the wrapping modes [99–101]. The lateral double quantum is also an attractive system as the transport through the system can be coherently manipulated by tuning the external flux threading the loop [91,92].

Eto [87] and Kuramoto [88] have studied theoretically the multi-level Kondo effects using the perturbative renormalisation group method (so called scaling theory) at equilibrium. They investigated the effects of the orbital degeneracy and the associated with SU(4) symmetry on the enhancement of the Kondo effect. More thorough theoretical investigations of the interplay of the orbital degeneracy and the SU(4) symmetry in the non-equilibrium transport regime have been given by [92] and [102] using the NRG method [43–49], non-crossing approximation (NCA) [103–105], equation-of-motion (EOM) [106] methods. It was also pointed out [102] that neither the enhanced Kondo temperature or the linear conductance measurement cannot distinguish between the SU(4) Kondo effect and the two-level SU(2) Kondo effect, which both give the same amount of the enhancement in the Kondo temperature; only the non-linear conductance at finite magnetic field has disguish the two effects unambiguously. In López et al. [92] it was found that the system undergoes a crossover between the SU(4) and the two-level SU(2) Kondo effects as changing the magnetic flux threading the loop.

Figure 8 Schematics of the prototype models exhibiting SU(4) Kondo effects. (a) Vertical quantum dot (b) Semiconducting carbon nanotube quantum dot (c) Double quantum dot. (d) Coupling scheme and (e) Coupling scheme corresponding to the double quantum dot in (c), which is mathematically equivalent to the scheme in (d); see the text

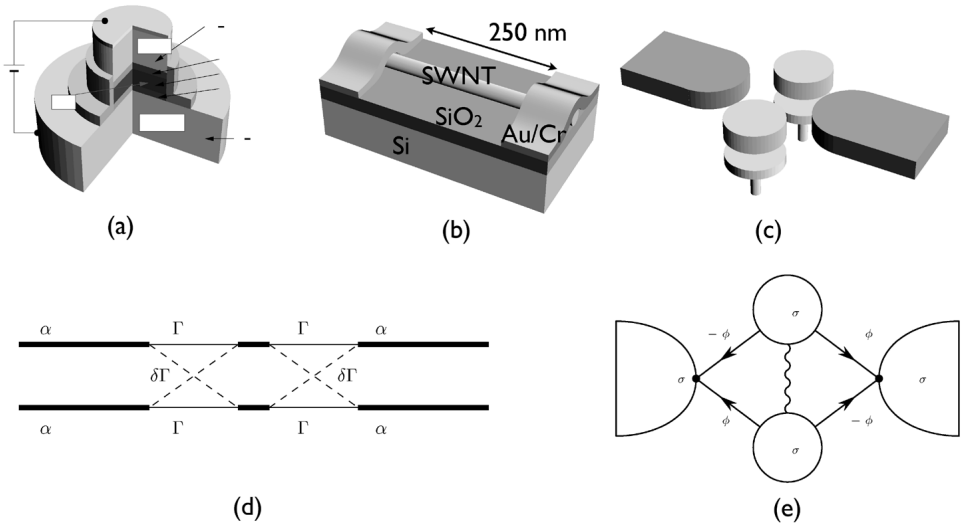

A strong enhancement of the Kondo effect has been reported in a recent experiment on vertical quantum dots [82]. Sasaki [82] found that the enhancement agreed qualitatively with the SU(4) model near the orbital degeneracy. While this experiment suggest strongly that the vertical quantum dot systems can exhibit SU(4) Kondo effects at the orbital degeneracy, in principle, the experimental data reported in this experiment can be explained in terms of the two-level SU(2) model. A more clearly evidence of the SU(4) Kondo effect associated with the orbital degeneracy was reported by Jarillo-Herrero et al [80,81] in experiments on carbon nanotube quantum dots in the presence of an external magnetic field parallel to the carbon nanotube axis. They observed the four-peak splitting of the Kondo resonance at finite magnetic field, a unique characteristic of the SU(4) Kondo effect [102].

Let us consider a system of quantum dots with two (nearly) degenerate localised orbitals. For a VQD, these orbitals correspond to two degenerate Fock-Darwin states with different values of the angular momentum quantum number. Sasaki et al [82] in the quantum dot. For a SWNT, they originate from the peculiar electronic structure of the nanotube. [81,101,107] The electronic states of a NT form one-dimensional electron and hole sub-bands as a result of the quantisation of the electron wavenumber perpendicular to the nanotube axis, $k_\perp$, which arises when graphene is wrapped into a cylinder to create a NT. By symmetry, for a given sub-band at $k_\perp = k_0$ there is a second degenerate sub-band at $k_\perp = -k_0$. Semiclassically, this orbital degeneracy corresponds to the clockwise (↻) or counterclockwise (↺) symmetry of the wrapping modes. In both cases the quantum number associated with the localised orbitals is related to the cylindrical symmetry of the 'dot'. Hereafter we will denote this orbital quantum number by $m = 1, 2$. In a parallel double QD, the degenerate orbital states are the lowest unoccupied states in two QDs, respectively. The 'dot' is then described by the Hamiltonian

$$H_D = \sum_{m=1,2} \sum_{\sigma=\uparrow,\downarrow} \varepsilon_{m\sigma} d^\dagger_{m\sigma} d_{m\sigma} + \sum_{(m,\sigma)\neq(m',\sigma')} U_{mm'} n_{m\sigma} n_{m'\sigma'}, \tag{6}$$

where $\varepsilon_{m\sigma}$ is the single-particle energy level of the localised state with orbital m and spin σ, $d^\dagger_{m\sigma}(d_{m\sigma})$ the fermion creation (annihilation) operator of the state, $n_{m\sigma} = d^\dagger_{m\sigma} d_{m\sigma}$ the occupation, $U_{mm}(m = 1, 2)$ the intra-orbital Coulomb interaction, and U_{12} the inter-orbital Coulomb interaction. The effect of the external magnetic field parallel to the symmetry axis of the system is to lifting the orbital and spin degeneracy of the single-particle energy levels. We will denote them by Δ_{orb} and Δz, respectively, so that the single-particle energy levels $\varepsilon_{m\sigma}$ has the form

$$\varepsilon_{m\sigma} = \varepsilon_0 + (2m-3)\Delta_{\text{orb}} + sign(\sigma)\Delta_Z/2. \tag{7}$$

The precise values of the Coulomb interactions $U_{mm'}$ depend on the details of the system, but should be of the order of the charging energy $E_C = e^2/2C$ with C being the total capacitance of the dot. In this work we focus on the regime where the system of the localised levels is occupied by a single electron ($\sum_{m\sigma}\langle n_{m\sigma}\rangle \approx 1$) and the Coulomb interaction energy ($U_{mm'} \sim E_C$) is much bigger than other energy scales. In this regime the Hamiltonian in equation (6) suffices to describe all relevant physics of our concern.

Kondo physics arises as a result of the interplay between the strong correlation in the dot and the coupling of the localised electrons with the itinerant electrons in conduction bands. Naturally, different Kondo effects are observed depending on the way the dot is coupled to the electrodes and whether the orbital quantum number m is conserved or not. Nevertheless, it turns out highly non-trivial *experimentally* to distinguish those different Kondo effects. In subsequent sections we will consider different coupling schemes between the dot and the electrodes, show how different physics emerges, and propose how to distinguish them unambiguously in experiments.

The two leads $\alpha = L$ and R are treated as non-interacting gases of fermions:

$$H_\alpha = \sum_k \sum_{\mu=1,2} \sum_\sigma \varepsilon_{\alpha k\mu}\, a^\dagger_{\alpha k\mu\sigma} a_{\alpha k\mu\sigma}, \tag{8}$$

where μ denotes the channels in the leads. Without loss of generality, we assume that there are two distinguished (groups of) channels $\mu = 1$ and 2 in each lead. When the leads bears the same symmetry as the dot, this channel quantum number μ in the leads is identical to the orbital quantum number m in the dot and will be preserved over the tunnelling of electrons from the dot to leads and vice versa; see Figure 8(d). Otherwise, there should occur the mixing of the channels and the orbitals; see Figure 8(d). The general situation is accounted by the tunnelling Hamiltonian

$$H_T = \sum_{\alpha k\mu\sigma} \left(V_{\alpha k\mu m\sigma} c^\dagger_{\alpha k\mu\sigma} d_{m\sigma} + h.c. \right). \tag{9}$$

The total Hamiltonian is then given by $H = H_L + H_R + H_T + H_D$. Notice that the parallel coupling of the double quantum dot to the two leads [see Figure 8(e)] can be shown to be mathematically equivalent to the Hamiltonian in equation (9).

For the sake of simplicity, we will assume identical electrodes ($\varepsilon_{Lk\mu} = \varepsilon_{Rk\mu}$), symmetric tunnelling junctions ($V_{Lk\mu m\sigma} = V_{Rk\mu m\sigma}$), and the tunnelling amplitudes independent of spin σ and the wave number k. Therefore it is convenient to consider a simplified model with $V_{\alpha k\mu m\sigma} = V_{\mu,m}/\sqrt{2}$. Then *in equilibrium* the Hamiltonian H in equation (8) is equivalent to $H = H_C + H_T + H_D$ with

$$H_C = \sum_{k\mu\sigma} \varepsilon_{k\mu} c^\dagger_{k\mu\sigma} c_{k\mu\sigma}, \tag{10}$$

$$H_T = \sum_{k\mu,m,\sigma} \left(V_{\mu m} c^\dagger_{k\mu\sigma} d_{m\sigma} + h.c. \right), \tag{11}$$

where we have made the canonical transformation

$$\begin{aligned} c_{k\mu\sigma} &= a_{Lk\mu\sigma} + a_{Rk\mu\sigma}, \\ b_{k\mu\sigma} &= a_{Lk\mu\sigma} - a_{Rk\mu\sigma}, \end{aligned} \tag{12}$$

and discarded the decoupled term $\varepsilon_{k\mu} b^\dagger_{k\mu\sigma} b_{k\mu\sigma}$.

At $B_\parallel = 0$, the spectral density shows a peak near the Fermi energy, corresponding to the formation of the SU(4) Kondo state; see Figure 9(a) (solid line). The peak width, which is much broader than that for the SU(2) Kondo model (dotted line), demonstrates the exponential enhancement of the Kondo temperature mentioned above. Another remarkable effect is that the SU(4) Kondo peak shifts away from $\omega = E_F = 0$ and is pinned at $\omega \approx T_K^{\mathrm{SU(4)}}$. This can be understood from the Friedel sum rule [108] which, in this case, gives $\delta = \pi/4$ for the scattering phase shift at E_F. Accordingly, the linear conductance at zero temperature is given by $G_0 = 4(e^2/h)\sin^2\delta = 2e^2/h$. It is interesting to recall that the Friedel sum rule gives the same linear conductance also for the TL SU(2) Kondo model. Thus, neither the enhancement of the Kondo temperature nor the linear conductance, can distinguish between the SU(4) and the TL SU(2) Kondo effects. This can only be achieved by studying the influence of a parallel magnetic field, which we do now.

Because of the underlying SU(4) symmetry, the orbital pseudo-spin should behave the same way as the real spin. In particular, the lift of the pseudo-spin degeneracy will split the Kondo peak (as long as the lift is larger than the Kondo temperature) just like the Zeeman splitting of the real spin does. The only difference is that pseudo-spin is more susceptible to the magnetic field than the real spin since $\mu_{\mathrm{orb}} \gg \mu_B$ (see above). Therefore, at sufficiently large fields $\left(2\Delta_{\mathrm{orb}} \gg \Delta_Z \gg T_K^{\mathrm{SU(4)}}\right)$, one has four split-Kondo peaks at $\omega \approx \pm 2\Delta_{\mathrm{orb}}$ and $\omega \approx \pm\Delta_Z$; see Figure 9. At moderate fields such that $2\Delta_{\mathrm{orb}} T_K^{\mathrm{SU(4)}} \gg T_K^{\mathrm{SU(2)}} \Delta_Z$, one can have a three-peak structure; see Figure 9(b) (dashed line). The lifted degeneracy in the orbital pseudo-spin gives two side-peaks at $\omega \approx \pm 2\Delta_{\mathrm{orb}}$ while the spin still retains a Kondo effect and gives the central peak. The central peak (which is now at $\omega = 0$) corresponds to a conventional SU(2) Kondo effect and hence is much narrower than the central resonance for $B_\parallel = 0$.

Figure 9 Local spectral density $A(\omega)$ for (a) $\Delta_{orb} = \Delta_Z = 0$ and (b, c) at finite magnetic fields. (a) and (b) are the NRG results and (c) is the EOM results

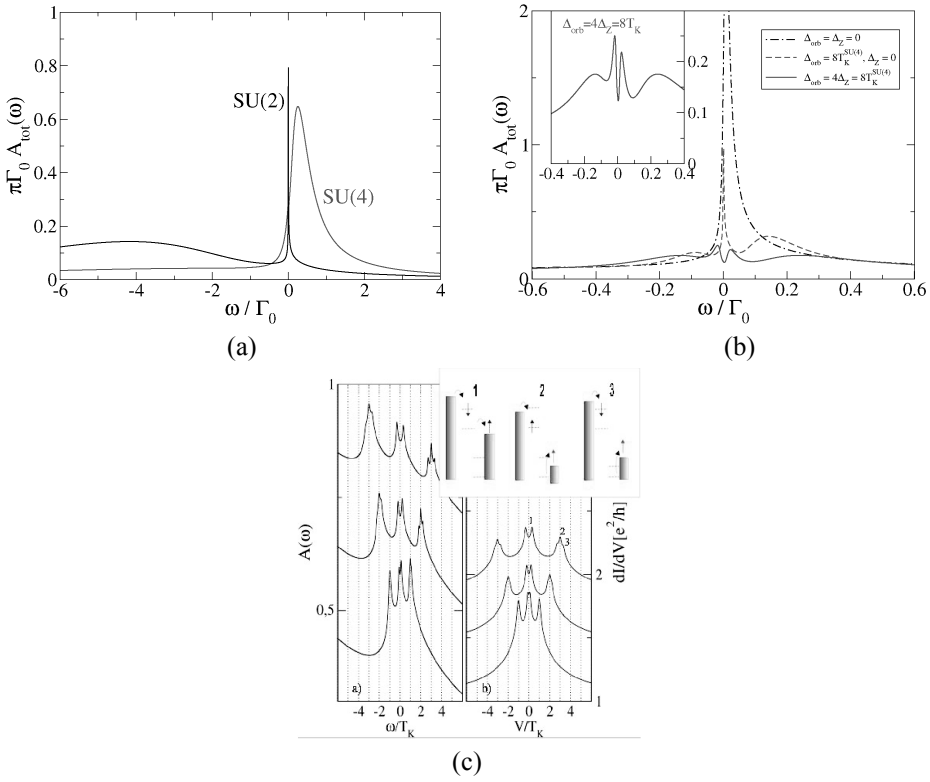

These features is ascribed essentially to the conservation of the orbital quantum number. Therefore, in the presence of the mixing between orbital quantum numbers will eventually destroy the SU(4) Kondo effects, leading to the less symmetric two-level SU(2) Kondo effects. One can see the crossover from the SU(4) to two-level SU(2) Kondo physics a function of the mixing parameter Γ_X/Γ_0 in Figure 10 By studying the dynamical susceptibility we find that the crossover occurs around $\Gamma_X/\Gamma_0 \approx 0.05$.

Figure 10 The total spectral density $A_d(E) = \sum_\sigma \sum_{mm'} \pi\Gamma_{mm'} A_{m'm;\sigma}(E)$ for different values of coupling asymmetry Γ_X/Γ_0

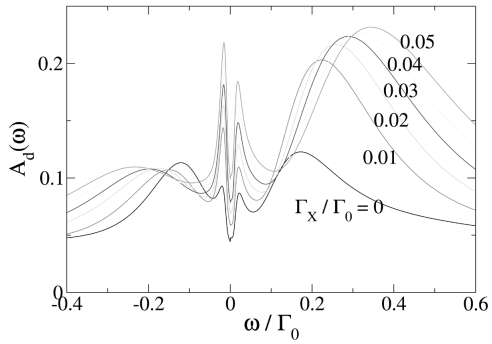

For the double quantum dot parallel coupled to the leads, one can tune the effective mixing between the two orbitals with the external magnetic flux. In Figure 11, one can see that T decreases as ϕ increases, which is consistent with the results of the SBMFT. Nevertheless, SBMFT overestimates the decreasing rate of the ZBA. The NRG results show that while the peak does not change appreciably for $\phi < \phi_c$, it decreases very rapidly for $\phi > \phi_c$.

Figure 11 Top panel: transmission probability vs. flux for (a) $\varepsilon_d = -7\Gamma$, $U_1 = U_2 = 5D$, $U_{12} = 0$, and (b) $\varepsilon_d = -14\Gamma$, $U_1 = U_2 = 5D$, and $U_{12} = 5D$. We set $\Gamma = D/60$. (Notice that we do not recover the unitary limit of T for $\phi \approx 0$ (mod 2π) because of the systematic errors introduced in the NRG procedure). Bottom panel ($U_{12} = 5D$): (c) Spin susceptibility (in an arbitrary unit) in the limit of strong interdot interaction. (d) The peak position of the susceptibility as a function of the flux ϕ

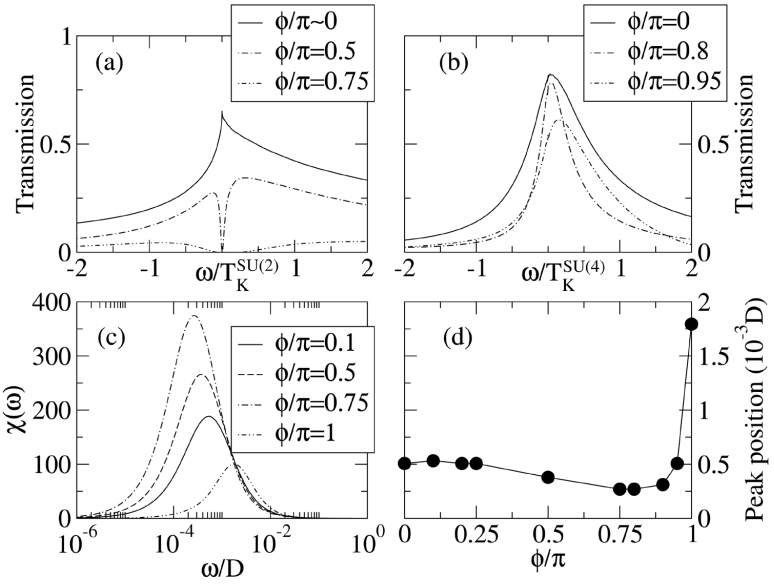

The value of ϕ_c is the last ingredient we have to explain. The ϕ_c marks the crossover between the SU(2) Kondo physics to the highly symmetric SU(4) Kondo state. Fortunately, ϕ_c can be extracted from the peak position of the spin susceptibility $\chi(\omega)$, which yields a reasonable estimate of the Kondo temperature. Figure 11(c) shows the evolution of χ when ϕ increases. Remarkably, when the flux enhances, at some point the position of the peak moves toward higher frequencies. The peak position as a function of ϕ is plotted in Figure 11(d). We observe that $T_K(\phi)$ is almost constant when ϕ goes from zero to $\phi \approx 0.75\pi$. This fact allows us to establish a criterium for the crossover between the SU(2) and SU(4) Kondo states in the double QD system.

5 Conclusions

A few selected topics on the Kondo effects in mesoscopic systems have been reviewed. The Kondo effects in quantum dots coupled to spin polarised ferromagnetic leads raised recently theoretical controversy. Through a thorough investigation based on the NRG, it

was suggested that the unitary Kondo limit is still available even at finite polarisation in the ferromagnetic leads if the system bears the particle-hole symmetry. The Kondo effects with ferromagnetic leads have been reported recently. In quantum dots coupled to superconducting leads, the Josephson current through the quantum dot in the Kondo regime and the $0 - \pi$ transition have attracted much interest recently. Due to the circular symmetry of the system in the vertical quantum dots and the carbon nanotube quantum dots, the orbital degrees of freedom also begin to play a role and interplay with the spin to give the SU(4) Kondo effects. The crossover between the SU(2) and SU(4) Kondo effects can be tuned with the external flux through the loop consisting of the double dots parallel coupled to two leads.

Acknowledgments

This work was supported by the SRC/ERC program of MOST/KOSEF (R11-2000-071), the Korea Research Foundation Grant funded by the Korean Government (KRF-2005-070-C00055), and the SK Fund. A part of the work was done while the author was visiting the Korea Institute for Advanced Study.

References and Notes

1 Hewson, A.C. (1993) *The Kondo Problem to Heavy Fermions*, Cambridge University Press, Cambridge.

2 Kondo, J. (1964) *Prog. Theor. Phys.*, Vol. 32, p.37.

3 Glazman, L.I. and Raĭkh, M.E. (1988) *Pis'ma Zh. Eksp. Teor. Fiz.*, Vol. 47, No. 8, p.378 [*JETP Lett*., (1988), Vol. 47, p.452].

4 Ng, T.K. and Lee, P.A. (1988) *Phys. Rev. Lett.*, Vol. 61, No. 15, p.1768.

5 Cronenwett, S.M., Oosterkamp, T.H. and Kouwenhoven, L.P. (1998) *Science*, Vol. 281, No. 5376, p.540.

6 Goldhaber-Gordon, D., Göres, J., Kastner, M.A., Shtrikman, H., Mahalu, D. and Meirav, U. (1998) *Phys. Rev. Lett.*, Vol. 81, No. 23, p.5225.

7 Goldhaber-Gordon, D., Shtrikman, H., Mahalu, D., Abusch-Magder, D., Meirav, U. and Kastner, M.A. (1998) *Nature* (London), Vol. 391, No. 6663, p.156.

8 Ji, Y., Heiblum, M., Sprinzak, D., Mahalu, D. and Shtrikman, H. (2000) *Science*, Vol. 290, No. 5492, p.779.

9 van der Wiel, W.G., De Franceschi, S., Fujisawa, T., Elzerman, J.M., Tarucha, S. and Kouwenhoven, L.P. (2000) *Science*, Vol. 289, No. 5487, p.2105.

10 Kouwenhoven, L. and Glazman, L. (2001) *Phys. World*, Vol. 14, No. 1, p.33.

11 Gerland, U., von Delft, J., Costi, T.A. and Oreg, Y. (2000) *Phys. Rev. Lett.*, Vol. 84, No. 16, p.3710.

12 Kang, K., Choi, M-S. and Lee, S. (2005) *Phys. Rev. B*, Vol. 71, No. 4, p.045 330.

13 Eto, M. and Nazarov, Y.V. (2001) *Phys. Rev. B*, Vol. 64, p.085 322.

14 Eto, M. and Nazarov, Y.V. (2002) *Phys. Rev. B*, Vol. 66, p.153 319.

15 Golovach, V.N. and Loss, D. (2003) *Europhys. Lett.*, Vol. 62, No. 1, p.83.

16 Izumida, W., Sakai, O. and Tarucha, S. (2001) *Phys. Rev. Lett.*, Vol. 87, No. 21, p.216 803.

17 Ng, T.K. and Lee, P.A. (2001) *Phys. Rev. Lett.*, Vol. 87, No. 21, p.216 601.

18 Pustilnik, M. and Glazman, L.I. (2001) *Phys. Rev. B*, Vol. 64, p.045 328.

19 Pustilnik, M., Avishai, Y. and Kikoin, K. (2000) *Phys. Rev. Lett.*, Vol. 84, No. 8, p.1756.

20 Sasaki, S., Franceschi, S.D., Elzerman, J.M., van der Wiel, W.G., Eto, M., Tarucha, S. and Kouwenhoven, L.P. (2002) *Nature* (London), Vol. 405, p.764.

21 Schmid, J., Weis, J., Eberl, K. and v. Klitzing, K. (2000) *Phys. Rev. Lett.*, Vol. 84, p.5824.

22 Affleck, I. and Simon, P. (2001) *Phys. Rev. Lett.*, Vol. 86, No. 13, p.2854.

23 Jones, B.A., Varma, C.M. and Wilkins, J.W. (1987) *Phys. Rev. Lett.*, Vol. 58, No. 9, p.843.

24 Bułka, B.R. and Lipiński, S. (2003) *Phys. Rev. B*, Vol. 67, p.024 404.

25 Choi, M-S., Sánchez, D. and López, R. (2004) *Phys. Rev. Lett.*, Vol. 92, No. 5, p.056 601.

26 Dong, B. *et al*. (unpublished) cond-mat/0302372.

27 López, R. and Sánchez, D. (2003) *Phys. Rev. Lett.*, Vol. 90, No. 11, p.116 602.

28 Lu, R. and Liu, Z. (unpublished) cond-mat/0210350.

29 Ma, J. *et al*. (unpublished) cond-mat/0212645.

30 Martinek, J. *et al*. (unpublished) cond-mat/0406323.

31 Martinek, J., Sindel, M., Borda, L., Barnaś, J., König, J., Schön, G. and von Delft, J. (2003) *Phys. Rev. Lett.*, Vol. 91, No. 24, p.202 247.

32 Martinek, J., Utsumi, Y., Imamura, H., Barnaś, J., Maekawa, S., König, J. and Schön, G. (2003) *Phys. Rev. Lett.*, Vol. 91, No. 12, p.127 203.

33 Pasupathy, A.N., Bialczak, R.C., Martinek, J., Grose, J.E., Doney, L.A.K., McEuen, P.L. and Ralph, D.C. (2004) *Science*, Vol. 306, p.86; Nygard, J., Koehl, W., Mason, N., DiCarlo, L. and Marcus, C. (unpublished) cond-mat/0410467.

34 Sánchez, D., López, R. and Choi, M-S. (2005) *J. Supercond.*, Vol. 18, No. 2, p.251, *Proceedings of The 3rd International Conference on Physics and Applications of Spin-Related Phenomena in Semiconductors (PASPS III)* (Santa Barbara, 21–23, July 2004).

35 Sergueev, N., Feng Sun, Q., Guo, H., Wang, B.G. and Wang, J. (2002) *Phys. Rev. B*, Vol. 65, p.165 303.

36 Zhang, P., Xue, Q-K., YupengWang and Xie, X. (2002) *Phys. Rev. Lett.*, Vol. 89, p.286 803.

37 Wolf, S.A., Awschalom, D.D., Buhrman, R.A., Daughton, J.M., von Molnár, S., Roukes, M.L., Chtchelkanova, A.Y. and Treger, D.M. (2001) *Science*, Vol. 294, p.1488.

38 Taniyama, T. *et al*. (2003) *Phys. Rev. Lett.*, Vol. 90, p.016 601.

39 Tsukagoshi, K., Alphenaar, B.W. and Ago, H. (1999) *Nature* (London), Vol. 401, p.572.

40 Nygård, J., Cobden, D.H. and Lindelof, P.E. (2000) *Nature* (London), Vol. 408, p.342.

41 Deshmukh, M.M. and Ralph, D.C. (2002) *Phys. Rev. Lett.*, Vol. 89, p.266 803.

42 Ng, T.K. (1993) *Phys. Rev. Lett.*, Vol. 70, p.3635.

43 Bulla, R., Costi, T.A. and Vollhardt, D. (2001) *Phys. Rev. B*, Vol. 64, p.45 103.

44 Costi, T.A. (2000) *Phys. Rev. Lett.*, Vol. 85, No. 7, p.1504.

45 Costi, T.A. and Hewson, A.C. (1993) *J. Phys.: Condens. Matt.*, Vol. 5, No. 30, p.L361.

46 Costi, T.A., Hewson, A.C. and Zlatic, V. (1994) *J. Phys.: Condens. Matt.*, Vol. 6, No. 13, p.2519.

47 Krishna-murthy, H.R., Wilkins, J.W. and Wilson, K.G. (1980) *Phys. Rev. B*, Vol. 21, No. 3, p.1003.

48 Krishna-murthy, H.R., Wilkins, J.W. and Wilson, K.G. (1980) *Phys. Rev. B*, Vol. 21, No. 3, p.1044.

49 Wilson, K.G. (1975) *Rev. Mod. Phys.*, Vol. 47, No. 4, p.773.

50 The contribution from finite Δ_Z to the spin-dependent Kondo peak is (almost) independent of Δ_K and can be used to compensate the latter; see [32] and [52].

51 Meir, Y. and Wingreen, N.S. (1992) *Phys. Rev. Lett.*, Vol. 68, No. 16, p.2512.

52 Choi, M-S., Hwang, N.Y. and Yang, S-R.E. (2003) *Phys. Rev. B*, Vol. 67, p.245 323.

53 This should not be confused with the behaviour of tunnel junctions with a *noninteracting* resonant level, where one usually has $g^{P} > g^{AP}$ and TMR increases with p [see, e.g., Bratkovsky, A.M. (1997) *Phys. Rev. B*, Vol. 56, p.2344)].

54 Bardeen, J., Cooper, L.N. and Schrieffer, J.R. (1957) *Phys. Rev.*, Vol. 106, p.162.

55 Shiba, H. and Soda, T. (1969) *Prog. Theor. Phys.*, Vol. 41, p.25.

56 Glazman, L.I. and Matveev, K.A. (1988) *Pis'ma Zh. Eksp. Teor. Fiz.*, Vol. 49, No. 10, p.570 [*JETP Lett.*, (1989) Vol. 49, No. 10, p.659].

57 Spivak, B.I. and Kivelson, S.A. (1991) *Phys. Rev. B*, Vol. 43, No. 4, p.3740.

58 Clerk, A.A. and Ambegaokar, V. (2000) *Phys. Rev. B*, Vol. 61, No. 13, p.9109.

59 Rozhkov, A.V. and Arovas, D.P. (1999) *Phys. Rev. Lett.*, Vol. 82, No. 13, p.2788.

60 Rozhkov, A.V. and Arovas, D.P. (2000) *Phys. Rev. B*, Vol. 62, No. 10, p.6687.

61 Vecino, E., Martín-Rodero, A. and Yeyati, A.L. (2003) *Phys. Rev. B*, Vol. 68, p.035 105.

62 Choi, M-S., Lee, M., Kang, K. and Belzig, W. (2004) *Phys. Rev. B*, Vol. 70, p.R020 502.

63 Choi, M-S., Lee, M., Kang, K. and Belzig, W. (2005) *Phys. Rev. Lett.*, Vol. 94, No. 22, p.229 701; cond-mat/0410415.

64 Oguri, A., Tanaka, Y. and Hewson, A.C. (2004) *J. Phys. Soc. Jpn.*, Vol. 73, No. 9, p.2494.

65 Yoshioka, T. and Ohashi, Y. (2000) *J. Phys. Soc. Jpn.*, Vol. 69, No. 6, p.1812.

66 Siano, F. and Egger, R. (2004) *Phys. Rev. Lett.*, Vol. 93, No. 4, p.047 002; *Erratum*, (2005) Vol. 94, p.039 902.

67 Siano, F. and Egger, R. (2004) *Phys. Rev. Lett.*, Vol. 94, p.229702.

68 Buitelaar, M.R., Nussbaumer, T. and Schönenberger, C. (2002) *Phys. Rev. Lett.*, Vol. 89, No. 25, p.256 801.

69 Haldane, F.D.M. (1978) *Phys. Rev. Lett.*, Vol. 40, No. 6, p.416; No. 13, p.911.

70 Beenakker, C.W.J. and van Houten, H. (1991) *Phys. Rev. Lett.*, Vol. 66, No. 23, p.3056.

71 Clerk, A.A., Ambegaokar, V. and Hershfield, S. (2000) *Phys. Rev. B*, Vol. 61, No. 5, p.3555.

72 Rozhkov, A.V., Arovas, D.P. and Guinea, F. (2001) *Phys. Rev. B*, Vol. 64, p.233 301.

73 Choi, M-S., Bruder, C. and Loss, D. (2001) in Averin, D.V., Ruggiero, B. and Silvestrini, P. (Eds.): *Macroscopic Quantum Coherence and Quantum Computing*, Kluwer Academic/Plenum Publishers, New York, p.307.

74 Choi, M-S., Bruder, C. and Loss, D. (2000) *Phys. Rev. B*, Vol. 62, No. 20, p.13 569.

75 Avishai, Y., Golub, A. and Zaikin, A.D. (2001) *Phys. Rev. B*, Vol. 63, p.134 515.

76 Levy Yeyati, A., Martín-Rodero, A. and Vecino, E. (2003) *Phys. Rev. Lett.*, Vol. 91, No. 26, p.266 802.

77 Tinkham, M. (1996) *Introduction to Superconductivity*, 2nd ed., McGraw-Hill, New York.

78 Sellier, G., Kopp, T., Kroha, J. and Barash, Y.S. (unpublished) cond-mat/0504649.

79 Bauer, A., Bentner, J., Aprili, M., Della Rocca, M.L., Reinwald, M., Wegscheider, W. and Strunk, C. (2004) *Phys. Rev. Lett.*, Vol. 92, p.217 001.

80 Jarillo-Herrero, P., Kong, J., van der Zant, H.S.J., Dekker, C., Kouwenhoven, L.P. and De Franceschi, S. (2005) *Phys. Rev. Lett.*, Vol. 94, p.156 802.

81 Jarillo-Herrero, P., Kong, J., van der Zant, H.S.J., Dekker, C., Kouwenhoven, L.P. and De Franceschi, S. (2005) *Nature*, Vol. 434, p.484.

82 Sasaki, S., Amaha, S., Asakawa, N., Eto, M. and Tarucha, S. (2004) *Phys. Rev. Lett.*, Vol. 93, No. 1, p.017 205.

83 Sasaki, S. and Tarucha, S. (2004) *J. Phys. Soc. Jpn.*, Vol. 74, No. 1, p.88, special issue on *Kondo Effect – 40 Years after the Discovery*.

84 Holleitner, A.W., Chudnovskiy, A., Pfannkuche, D., Eberl, K. and Blick4, R.H. (2004) *Phys. Rev. B*, Vol. 70, p.075 204.

85 Jeong, H. *et al*. (2001) *Science*, Vol. 293, p.2221.

86 Wilhelm, U. and Weiss, J. (2000) *Physica E*, Vol. 6, p.668.

87 Eto, M. (2004) *J. Phys. Soc. Jpn.*, Vol. 74, No. 1, p.95, special issue on *Kondo Effect – 40 Years after the Discovery*.

88 Kuramoto, Y. (1998) *Eur. Phys. J. B*, Vol. 5, p.457.

89 Pohjola, T., König, J., Salomaa, M.M., Schmid, J., Schoeller, H. and Schön, G. (1997) *Europhys. Lett.*, Vol. 40, No. 2, p.189.

90 Pohjola, T., Schoeller, H. and Schön, G. (2001) *Europhys. Lett.*, Vol. 54, No. 2, p.241.

91 Borda, L., Hofstetter, G.Z.W., Halperin, B.I. and von Delft, J. (2003) *Phys. Rev. Lett.*, Vol. 90, No. 2, p.026 602.

92 López, R., Sánchez, D., Lee, M., Choi, M-S., Simon, P. and Le Hur, K. (2005) *Phys. Rev. B*, Vol. 71, p.115 312.

93 Zaránd, G., Brataas, A. and Goldhaber-Gordon, D. (2003) *Solid State Commun.*, Vol. 126, p.463.

94 Oosterkamp, T.H., Janssen, J.W., Kouwenhoven, L.P., Austing, D.G., Honda, T. and Tarucha, S. (1999) *Phys. Rev. Lett.*, Vol. 82, No. 14, p.2931.

95 Liang, W. *et al*. (2001) *Nature*, Vol. 411, p.665.

96 Bockrath, M., Cobden, D.H., Lu, J., Rinzler, A.G., Smalley, R.E., Balents, L. and McEuen, P.L. (1999) *Nature* (London), Vol. 397, No. 6720, p.598.

97 Liang, W., Bockrath, M. and Park, H. (2002) *Phys. Rev. Lett.*, Vol. 88, No. 12, p.126 801.

98 Liang, W. *et al*. (2002) *Nature*, Vol. 417, p.725.

99 Ajiki, H. and Ando, T. (1993) *J. Phys. Soc. Jpn.*, Vol. 62, p.1255.

100 Lu, J.P. (1995) *Phys. Rev. Lett.*, Vol. 74, p.1123.

101 Minot, E.D., Yaish, Y., Sazonova, V. and McEuen, P.L. (2004) *Nature* (London), Vol. 428, p.536.

102 Choi, M-S., López, R. and Aguado, R. (2005) *Phys. Rev. Lett.*, Vol. 95, p.067204.

103 Hettler, M.H., Kroha, J. and Hershfield, S. (1998) *Phys. Rev. B*, Vol. 58, p.5649.

104 Langreth, D.C. and Nordlander, P. (1991) *Phys. Rev. B*, Vol. 43, No. 4, p.2541.

105 Wingreen, N.S. and Meir, Y. (1994) *Phys. Rev. B*, Vol. 49, No. 16, p.11 040.

106 We combine occupations obtained from a non-equilibrium $U \to \infty$ NCA calculation with EOM retarded Green's function and include the finite lifetime of the intermediate states due to cotunnelling at finite voltages and/or magnetic fields. See, Meir, Y., Wingreen, N.S. and Lee, P.A. (1993) *Phys. Rev. Lett.*, Vol. 70, p.2601.

107 Cao, J., Wang, Q., Rolandi, M. and Dai, H. (2004) *Phys. Rev. Lett.*, Vol. 93, No. 21, p.216 803.

108 Langreth, D.C. (1966) *Phys. Rev.*, Vol. 150, No. 2, p.516.